

1
2
3
4
5
6
7
8
9
10
11
12
13
14
15
16
17
18
19
20
21
22
23
24
25
26
27
28

MR. DAVID F MUÑOZ (Orcid ID : 0000-0001-6032-1082)

DR. ROHAM BAKHTYAR (Orcid ID : 0000-0003-0506-6706)

Article type : Technical Paper

Extreme water level simulation and component analysis in Delaware Estuary during Hurricane Isabel

Dongxiao Yin, David F. Muñoz, Roham Bakhtyar, Z. George Xue, Hamed Moftakhari, Celso Ferreira and Kyle Mandli

Department of Oceanography and Coastal Sciences (Yin, Xue), Louisiana State University, Baton Rouge, Louisiana, USA; Department of Civil, Construction and Environmental Engineering (Muñoz, Moftakhari), The University of Alabama, Tuscaloosa, Alabama, USA; U.S. Army Corps of Engineers (USACE, Bakhtyar), Southwestern Division, Galveston, Texas, USA; National Water Center (Bakhtyar previously at), NOAA/NWS/OWP, Tuscaloosa, Alabama, USA; Center for Computation and Technology(Xue), Louisiana State University, Baton Rouge, Louisiana, USA; Coastal Studies Institute(Xue), Louisiana State University, Baton Rouge, Louisiana, USA; Civil, Infrastructure and Environmental Engineering Department (Ferreira), George Mason University, Fairfax, Virginia, USA; Applied Physics and Applied Mathematics Department (Mandli), Columbia University, New York, New York, USA. (Correspondence to Yin: dyin2@lsu.edu).

Research Impact Statement: A model framework taking advantage of National Water Model, D-Flow FM and ADCIRC for water level simulation over coastal transition zone during hurricane events is built. It can satisfactorily simulate the extreme water level with an average Willmott skill of 0.965 over Delaware Estuary during Hurricane Isabel (2003).

ABSTRACT:

This is the author manuscript accepted for publication and has undergone full peer review but has not been through the copyediting, typesetting, pagination and proofreading process, which may lead to differences between this version and the [Version of Record](#). Please cite this article as [doi: 10.xxxx/jawr.12947](#)

29 Sea level rise and intense hurricane events make East and Gulf Coasts of the United States
30 increasingly vulnerable to flooding, which necessitates the development of computational
31 models for accurate water level simulation in these areas to safeguard the coastal wellbeing.
32 With this regard, a model framework for water level simulation over coastal transition zone
33 during hurricane events is built in this study. The model takes advantage of National Water
34 Model's strength in simulating rainfall-runoff process, and D-Flow Flexible Mesh's ability to
35 support unstructured grid in hydrodynamic processes simulation with storm surges/tides
36 information from the Advanced CIRCulation model. We apply the model on Delaware Estuary
37 to simulate extreme water level and to investigate the contribution of different physical
38 components to it during Hurricane Isabel (2003). The model shows satisfactory performance
39 with an average Willmott skill of 0.965. Model results suggest that storm surge is the most
40 dominating component of extreme water level with an average contribution of 78.16%, second
41 by astronomical tide with 19.52%. While the contribution of rivers is mainly restricted to the
42 upper part of the estuary upstream of Schuylkill River, local wind induced water level is more
43 pronounced with values larger than 0.2m over most part of the estuary.

44 (KEYWORDS: National Water Model; D-Flow FM; ADCIRC; extreme water level, Delaware
45 Estuary)

46 INTRODUCTION

47 Flood is a natural hazard characterized by the overflowing of large amounts of water
48 beyond normal thresholds. As the most destructive natural hazard, floods have caused 157,000
49 fatalities and significant economic losses around the world during 1995 to 2015 (Disasters,
50 Centre for Research on the Epidemiology of Reduction, 2015). In the United States of America,
51 floods are responsible for more fatalities than any other natural disasters. For the past 3 decades,
52 freshwater flooding has caused an annual average of \$8.2 billion in damage (Wing *et al.*, 2018).
53 The 2016 Louisiana flood alone damaged 60,000 homes and caused 13 deaths, bringing about a
54 total economic loss of \$10 billion (Vahedifard *et al.*, 2016; Wing *et al.*, 2018).

55 Based on the occurring location and dominating mechanism, floods can be generally
56 classified into 3 categories: fluvial flood, pluvial flood (or flash flood), and coastal flood, which
57 is commonly found in large river with wetter climate, dry areas with a dry climate under
58 excessive rainfall and coastal areas subjected to storm surge penetration, respectively. Each type

59 of flood has been studied over different scales and locations by researchers using either
60 observation or simulation methods (e.g., Merz *et al.*, 2010 for fluvial flood; Saharia *et al.*, 2017
61 for flash flood; Winsemius *et al.*, 2016 for fluvial flood and Wdowinski *et al.*, 2016 for coastal
62 flood). Besides the three types of floods characterized by one single driving force, there is also
63 compound flood, which is the result of the combined effect of two or more driving factors
64 (Moftakhari *et al.*, 2017). The coastal to inland transition zone acts as a “hotspot” for compound
65 flood to happen (Bilskie and Hagen, 2018). Under catastrophic weather events such as hurricanes,
66 torrential precipitation, storm surge and rainfall-runoff process interact with each other over the
67 coastal transition zone, resulting in extreme water level that can cause substantial economic and
68 human losses.

69 With over 50% of the total population residing in coastal regions (Moftakhari *et al.*, 2015)
70 and the rising sea level and increasing average intensity of hurricane (Webster *et al.*, 2005;
71 Woodruff *et al.*, 2013), the contiguous United States, especially the Gulf and East Coasts, are
72 becoming increasingly vulnerable to extreme water level. Thus, accurate forecast of extreme
73 water levels over these areas during hurricane events is of critical importance and desperately
74 needed. However, conventional methods that focus on one driver at a time may under-
75 /overestimate the risk associated with such floods (Moftakhari *et al.*, 2019). With this regard, the
76 National Oceanic and Atmospheric Administration (NOAA) National Water Center (NWC)
77 initiated the research project to build a numerical framework for accurate water level simulation
78 in coastal transition zone. Under this project, considerable efforts have been devoted to select,
79 design and test different modeling frameworks with available hydrological and hydrodynamic
80 models (e.g., Bakhtyar *et al.*, 2019, 2020; Muñoz *et al.*, 2020 in process).

81 To accurately simulate the extreme water level over coastal transition zone under hazardous
82 weather events, both hydrological and oceanic processes need to be considered in the model
83 framework. Usually, a hydrologic and a hydrodynamic component is coupled in either offline or
84 online mode. For instance, using the Soil and Water Assessment Tool (SWAT, Arnold, J. G.,
85 Srinivasan, R., Muttiah, R. S., & Williams, 1998) together with the ADvanced CIRCulation
86 model (ADCIRC, Luetlich *et al.*, 1993), Bacopoulos *et al.*, (2017) studied the extreme water
87 level over the St. Johns River Basin during Tropical Storm Fay in 2018. SWAT and ADCIRC
88 were integrated in the way that runoff hydrographs from SWAT were introduced into ADCIRC
89 as river inflow boundary condition. Similarly, Dresback *et al.*, (2013) built a modeling system

90 named ASGS-STORM (Scalable Terrestrial, Ocean, River and Meteorological ADCIRC Surge
91 Guidance System), which uses Hydrology Laboratory-Research Distributed Hydrologic Model
92 (Koren *et al.*, 2004) and ADCIRC as the hydrologic and hydrodynamic component respectively.
93 The system was tested on Hurricane Irene for three advisories (Advisory 23, 25 and 28) and the
94 best track from the National Hurricane Center. While the model showed overestimation for two
95 of the advisories (Advisory 23 and 25), it well simulated total water level, wind speed and wind
96 direction when using Advisory 28 along with the best track. However, most of the hydrological
97 components used in previous studies are either lumped models or grid-based models with coarse
98 resolutions (e.g., 4km in ASGS-STORM). In the lumped models, the computational domain is
99 usually divided into a series of basic hydrologic units such as hillslope or channel. Over each
100 hydrologic unit, hydrologic parameters are uniformly distributed. This makes the model unable
101 to take into consideration of the spatial heterogeneity of the flood response. In addition, the grid-
102 based model with coarse resolution may fail to resolve the flash flood process at finer scale.

103 As part of efforts motivated by NWC's initiative and an extension of previous studies,
104 this study introduces a numerical framework capable of simulating the extreme water level over
105 coastal transition zone under hurricane conditions. We apply it on the Delaware Estuary during
106 Hurricane Isabel (2003) to investigate the relative contribution of different physical components
107 to extreme water levels. The rest of the paper is organized as follows. Study area, data, model
108 framework and numerical experiments conducted as well as the statistical metrics applied in this
109 study are detailed in Methods. In Results, the simulated astronomical tide, streamflow, wind field
110 and total water level are presented and validated. Following model results, the contribution and
111 spatial distribution of different physical components of total water level are discussed and model
112 uncertainty is analyzed. A conclusion is given in the last section.

113 METHODS

114 *Study Area, Study Event and Data*

115 The Delaware Estuary is a coastal plain estuary located on the East Coast of the United
116 States surrounded by the States of Delaware, New Jersey and Pennsylvania. It extends from the
117 river mouth at Cape May all the way upstream to the head of the tide at Trenton, New Jersey,
118 with a drainage basin of around 35,000 km², a length of 215km and an average depth of 8m
119 (Sharp *et al.*, 1986; Walters, 1997). Among all the rivers flowing into the estuary, the Delaware

120 River provides almost 58% of the total discharge, followed by the Schuylkill River contributing
121 15%. No other single river is responsible for more than 1% of the total discharge beyond these
122 two rivers (Sharp, 1983). The river discharge varies seasonally, which is relatively low during
123 summer and autumn and high in spring. During normal discharge conditions, the Delaware
124 Estuary is vertically homogeneous, and water motion in the estuary is dominated mainly by tidal
125 current. However, stratification can exist when spring freshet occurs. The tides in the Delaware
126 Estuary are semidiurnal, with principal lunar semidiurnal constituent (M_2) the dominating
127 constituent. In addition to tides and river discharge, the estuary circulation is also influenced by
128 meteorological effects, especially when it experiences landfalling hurricanes.

129 Hurricane Isabel was the deadliest and most intense hurricane in the 2003 Atlantic
130 Hurricane Season. As is shown in Figure 1b, it formed on 1200 UTC September 7, 2003 and
131 strengthened into a Category 5 hurricane four days later at 1800 UTC September 11. It made
132 landfall as a Category 2 Hurricane around 1700 UTC September 18 near Drum Inlet, North
133 Carolina (Beven and Cobb, 2003). Multiple hazards, including heavy rainfall, flooding, storm
134 surge and wind damage, were caused by Isabel, resulting in 34 deaths and more than \$3.3 billion
135 in economic losses (Beven and Cobb, 2003; Lin *et al.*, 2010; Sheng *et al.*, 2010).

136 Water levels, wind speed, pressure and river discharge observation data were collected in
137 this study to validate the model performance. Water level observation data was obtained from the
138 Center for Operational Oceanographic Products and Services (CO-OPS, “NOAA Tides and
139 Currents”). Wind speed and pressure data was collected from a buoy station of the National Data
140 Buoy Center (NDBC, “National Data Buoy Center”). River discharge observations were
141 obtained from the U.S. Geological Survey (USGS, “USGS Water Data for the Nation”). The
142 locations of the CO-OPS stations, USGS gauges and NDBC Buoy station are shown in Figure 1c.

143 *Model Framework*

144 Figure 1a shows the schematic structure of the model framework used in this study. Each
145 component in the model framework is coupled in offline mode. The NOAA National Water
146 Model (NWM) serves as the hydrologic component responsible for simulating rainfall-runoff
147 process and providing river discharge information. Beyond the estuary in the open ocean,
148 ADCIRC is employed to prepare the open boundary conditions. The local meteorological forcing
149 over the estuary is from Climate Forecast System Reanalysis (CFSR, National Center for

150 Atmospheric Research Staff (Eds), Last modified 08 Nov 2017). Finally the D-Flow Flexible
151 Mesh (D-Flow FM , Deltares, 2019a) model ingests boundary conditions and local
152 meteorological forcing to simulate the dynamical processes in the coastal transition zone.

153 Each component in this framework has been previously calibrated. The D-Flow FM and
154 ADCIRC have been calibrated and validated by Bakhtyar et al., (2019, 2020) over the study area
155 during Hurricane Isabel. Readers are referred to Bakhtyar et al., (2019, 2020) for the detail of the
156 calibration process. NWM is calibrated by the National Water Center and WRF-Hydro
157 developing team. A 10-year spin up was conducted for the model to reach equilibrium condition
158 and a 1-year spin up is chosen prior to formal calibration (Rafieeiniasab *et al.*, 2020).

159 **Hydrologic component:** NWM is a hydrologic modelling framework operated at NOAA's
160 National Water Center providing streamflow forecasts at 2.7 million river reaches over the entire
161 continental United States. The core component of the NWM is the community Weather Research
162 and Forecasting model Hydrological modeling system (WRF-Hydro, Gochis *et al.*, 2018). It
163 utilizes the Noah land surface model with multi-parameterization options (Noah-MP, Niu *et al.*,
164 2011) to simulate the land surface process. With meteorological forcing data from a variety of
165 sources, rainfall-runoff processes are first performed on Noah-MP with a grid resolution of 1km.
166 Upon that, subsurface and surface flow are routed laterally on the same domain with a higher
167 horizontal resolution determined by a disaggregation factor. In the NWM, the disaggregation
168 factor is 4, corresponding to the grid size of 250m, making it capable of resolving flash flooding
169 at finer scales. Once the overland flow gets into the channel network, a Muskingum-Cunge
170 channel routing method is employed to rout the streamflow on the stream reaches delineated in
171 National Hydrography Dataset Plus V2 (McKay *et al.*, 2019).

172 In this study, the NWM was used to simulate the rainfall-runoff and channel flow
173 processes upstream of the Delaware Estuary. The simulated streamflow/river discharge time
174 series provided by the National Water Center were integrated into the D-Flow FM model at 11
175 river inputs along the boundary (Figure 1c).

176 **Hydrodynamic component:** D-Flow FM is the successor of the Delft 3D-FLOW
177 (Deltares, 2019b). Both models implement a finite volume method to solve the shallow water
178 equations on staggered unstructured grids, which allow for the coexistence of both curvilinear
179 grids as well as triangles, quads, pentagons and hexagons. In this study D-Flow FM is run in 2D
180 mode while 1D, 1D-2D combination, and 3D mode are also supported. The computational mesh

181 (Figure 1c, yellow area) covers the entire Delaware Estuary, which extends from the estuary
182 mouth all the way to Trenton, New Jersey. It consists of 34,387 nodes and 72,435 netlinks,
183 which are the edges connecting nodes. The resolution of the mesh varies from 6m up to 1.2km.
184 The initial timestep is 1s and maximum timestep is 60s, which are default values in D-Flow FM.
185 Small initial timestep can make sure model starts smoothly. During simulation, the
186 computational timestep increases from the initial timestep to the values limited by Courant–
187 Friedrichs–Lewy condition whose maximum value is set to 0.75. The horizontal and vertical
188 datum applied in the model is the World Geodetic System (WGS-84) and North American
189 Vertical Datum of 1988 (NAVD88), respectively. The open boundary conditions are passed from
190 ADCIRC running in the open ocean while river discharge input is from the NWM reanalysis as
191 boundary conditions. The meteorological forcing is from CFSR generated by the National
192 Centers for Environmental Prediction (NCEP), which is a third-generation reanalysis product
193 with a resolution around 38km.

194 The major feature of this model framework is using D-Flow FM as the intermediate
195 component to simulate the hydrodynamic processes in the coastal transition zone, instead of
196 employing ADCIRC or Delft 3D-FLOW alone as the hydrodynamic component in previous
197 studies. This is mainly due to the consideration of this model framework’s potential use over all
198 the coastal areas of the United States in NWC, where accuracy as well as computational
199 efficiency are the two major concerns. With D-Flow FM’s strength in supporting 1D-2D
200 combination mesh as well as unstructured grids, it can generate the modeling mesh with optimal
201 flexibility according to the physical setting of target area. In this case, computational efficiency
202 as well as required accuracy is expected to be achieved in a better way than previous models. In
203 this study, infiltration scheme of D-Flow FM was not activated since the infiltration amount over
204 the Delaware Estuary is considered negligible during the simulation period. This setup is
205 regarded as reasonable because the estuary is permanent water cover area and the bed soils
206 should be saturated, which leaves little space for infiltration to occur. Beyond the domain of D-
207 Flow FM on the land side, the infiltration process was simulated by the NWM through its land
208 surface component Noah-MP with an infiltration excess algorithm.

209 **ADCIRC** is an open source numerical ocean circulation model widely used by researchers in
210 simulating extreme water level under hurricane events(e.g., Bacopoulos *et al.*, 2017; Dresback *et*
211 *al.*, 2013; Marsooli and Lin, 2018). With the hydrostatic assumption and the standard Boussinesq

212 approximation, it solves the governing equations using a finite element method in space and
213 finite difference method in time. In this study, ADCIRC was used beyond the Delaware Estuary
214 in the ocean to provide open boundary conditions for D-Flow FM. The simulation of ADCIRC is
215 carried out on an unstructured mesh with ~1.8 million nodes and the lowest resolution is around
216 200 m near the coast (Bakhtyar *et al.*, 2020).

Author Manuscript

[Insert Figure 1]

Experiment Design

To achieve the study objective, 4 experiments (namely E1 through E4) under 4 different scenarios were designed and carried out. The details of the setup of the experiments are shown in Table 1. In E1, tide signal was calculated by ADCIRC and sent to D-Flow FM via the open boundary. The water level simulated in E1 represents the astronomical tide. Based on E1, the river discharge information was added through the land boundary into the model. Thus, the simulated water level in E2 contains the astronomical tide as well as the river discharge induced water level component. Similarly, E3 simulates the water level induced by astronomical tide in combination with local wind forcing. In E4, the water level signal including storm surge and tides simulated by ADCIRC was introduced into the D-Flow FM as the open boundary condition. The effects of river discharge and local wind forcing were also considered. Thus, the total water level was simulated in this experiment. It is noted that, due to the absence of wave component in the model framework, the water level simulated in this study does not contain wave setup/set-down induced water level component. Also, the storm surge induced water level simulated in this study contains both the surge induced water level and the tide-surge interaction induced component.

For E1, the simulation was carried out from 12 to 25 September 2003 for 13 days with the first day for spin-up. For E2, E3, E4 the model started from 29 August 2003, and ended on 25 September 2003. The first 13 days of simulation were taken for spin-up considering longer time needed for the meteorological forcing to reach an equilibrium state. All model simulations were conducted with an Intel Core i7-7700 - 3.60 GHz CPU and 64 GB RAM.

Model Evaluation

To quantitatively evaluate the simulated water level, the statistical metrics including R-square (R^2), root mean square error (RMSE), bias, and Willmott skill are calculated. R-square is the square of the Pearson correlation coefficient, which is the ratio between the sample covariance and the product of the standard deviations from the observed and simulated values. RMSE is the squared root of the mean square error. The perfect score is zero. Bias is used to evaluate the model's tendency to over- or under-estimate simulated variables. Willmott skill

(Willmott, 1981) is used to evaluate the modeling performance, ranging from 0 to 1, with higher values indicating better performance. These skills are defined as

$$R^2 = \left(\frac{\sum_1^N (X_{sim} - \overline{X_{sim}})(X_{obs} - \overline{X_{obs}})}{\sqrt{\sum_1^N (X_{sim} - \overline{X_{sim}})^2 * \sum_1^N (X_{obs} - \overline{X_{obs}})^2}} \right)^2 \quad (1)$$

$$RMSE = \sqrt{\frac{\sum_1^N (X_{sim} - X_{obs})^2}{N}} \quad (2)$$

$$Bias = \frac{\sum_1^N (X_{sim} - X_{obs})}{N} \quad (3)$$

$$Skill = 1 - \frac{\sum_1^N |X_{sim} - X_{obs}|^2}{\sum_1^N (|X_{sim} - \overline{X_{obs}}| + |X_{obs} - \overline{X_{obs}}|)^2} \quad (4)$$

where X represents the variable being compared, N is the number of the data points.

RESULTS

Astronomical tide

Astronomical tide is one of the major components of total water level in Delaware Estuary. Accurately simulating the total water level then implies that the astronomical tide should also be accurate in the model. In this study, the astronomical tide was simulated in E1. The simulated tide is compared against NOAA tide prediction at seven CO-OPS tidal gauges (Figure 1c). It should be noted that the NOAA tide prediction data at gauges except Lewes and Cape May are based on mean sea level (MSL) instead of North American Vertical Datum of 1988 (NAVD 88), which is used in this study. In this case, to facilitate the comparison, the NOAA prediction data was first transformed from MSL based to NAVD 88 based using vertical datum transformation tool (“NOAA/NOS’s VDatum 4.0.1: Vertical Datums Transformation”) developed by NOAA. The transformation relationships are shown in Table 2.

In Figure 2 we compare the simulated astronomical tide with NOAA tide predictions at the selected CO-OPS gauges. Model simulation and NOAA prediction are in good agreement. The R^2 , Bias, RMSE and Willmott skill at the seven tidal gauges are 0.984, 0.105 (absolute value), 0.15 and 0.98 on average. This reveals that our model satisfactorily captures the tides in the study area.

[Insert Figure 2]

Atmospheric pressure and wind

Local meteorological conditions including wind and atmospheric pressure can influence the water level in the Delaware Estuary. During storm surge events, low pressure in addition to strong wind can highly affect the estuary circulation. In this study, the wind and atmospheric pressure forcing used to drive D-Flow FM is from CFSR. To evaluate CFSR's performance in our study area, the atmospheric pressure and wind fields of CFSR is compared against the observation data at NDBC buoy station 44009 (Figure 1c). As shown in Figure 3, CFSR shows satisfactory performance in simulating wind speed and atmospheric pressure with high coefficient, low bias and high skill. And the simulated wind direction agrees well with the observed one despite some discrepancies partly due to the different averaging periods used in model and observation.

[Insert Figure 3]

River discharge

As the Delaware River and the Schuylkill river are the two most important river discharges into the Delaware Estuary, we assume that good performance of the NWM on these two rivers should indicate satisfactory performance of the hydrologic component over the whole study area. In Figure 4 we compare the simulated river discharge against the observations at corresponding USGS Gages (Figure 1c). Overall, the hydrological model can capture the timing and magnitude of the hydrographs during Hurricane Isabel while overestimation can be found after September 23. Nevertheless, as our analysis mainly focuses on the one-week window around the landfall of Isabel (September 15 to September 23), such observations should not influence the primary analysis. It should be noted that observation data is not available for the Delaware River during September 10 to September 15, 2003, warranting the necessity of using a hydrological model to provide continuous discharge data during the extreme event.

[Insert Figure 4]

Total water level

In this study, the total water level was simulated in E4, with contributions from tide, rivers, local wind forcing and storm surge from the open ocean. However, the water level

component from wave setup and set-down is not considered due to the absence of wave model components over the Delaware Estuary in the model framework.

Simulated total water level is compared against the observation at selected CO-OPS gauges in Figure 5. Overall, the model can reproduce well the total water level during the simulation period, with the averaged (seven stations) R^2 , Bias, RMSE and Willmott skill value of 0.955, 0.073 (absolute value), 0.2, and 0.970, respectively

In addition to the total water level, we further validated model performance in extreme water levels simulation. The extreme water levels at each tidal gauge were picked out according to the observation and were compared against the corresponding simulated values (Figure 6). The comparison reveals that the model has satisfactorily simulated the extreme water level during Isabel with high R^2 , high Willmott skill, low Bias and relatively low RMSE.

[Insert Figure 5]

[Insert Figure 6]

DISCUSSION

In this study, storm surge induced water level is generated by subtracting the result of E2 from that of E4. River discharge induced water level components are calculated by subtracting the astronomical tide simulated in E1 from the water level simulated in E2. Similarly, the water level components caused by local wind forcing is the difference between the water level in E3 and the astronomical tides from E1. It is noted that the storm surge component presented here contains the water level component induced by surge signal passed from an ocean boundary as well as the one caused by local meteorological forcing. In addition, tidal-surge iteration induced water level fluctuation is not separated from the purely surge component, which is discussed below.

Extreme water level component analysis

The respective contribution of storm surge, astronomical tide, and river discharge to the extreme water level at the selected CO-OPS gauges is shown in Figure 7. The simulated extreme water level increases from 1.132m at the lower part of the estuary to 2.569m in the upstream. Storm surge is the most dominating component at all the gauges accounting for 78.16% of the extreme water level on average, followed by astronomical tide with an average contribution of 19.52%. While the astronomical tide contribution is significant at lower part of the Delaware

Estuary (tidal gauges downstream of Brandywine Shoal Light), it becomes minimal in the middle reach of the estuary (tidal gauges Ship John Shoal and Marcus Hook) and turns prominent again further upstream (tidal gauges Burlington and Newbold). This change of astronomical tide's contribution to total water level implies that storm surge has coincided with positive tide level at the lower and upper part of the estuary, while with negative tide level in the middle reach of the estuary. The riverine contribution to extreme water level is mainly limited to the area upstream of Marcus Hook, which should mainly be attributed to the Delaware River. Downstream of Ship John Shoal, rivers show almost no contribution to the extreme water level, implying the minimal impact of river input to the water level in the lower part of the Delaware Estuary.

[Insert Figure 7]

Extreme water level and maximum storm surge

Figure 8 shows the spatial distribution of simulated extreme water level and the storm surge induced water level maximum over the study area during September 15 to September 23. Overall, the simulated extreme water level (Figure 8a) increases along the longitudinal direction in the estuary, which is mainly attributed to the piling up of water driven by storm surge as well as the funneling effect due to the narrowing of the channel width upstream. In the lateral direction, over the lower part of the Delaware Estuary, the 1.4m isobath deflects to the left side when looking upstream indicating that the extreme water level on the New Jersey side is higher than that of the Delaware side. This lateral difference can be ascribed to the southeast-to-northwest and south-to-north movement of water driven by the northerly and northwesterly wind after Isabel's landfall (Figure 3a, 3b) as well as the Coriolis effect (Sharp, 1983). The maximum storm surge component (Figure 8b) exhibits similar spatial pattern with the extreme water level, implying the dominating influence of storm surge to extreme water level during Hurricane Isabel. Figure 8c details the difference between extreme water level and maximum storm surge over the study area. From the mouth of Delaware Estuary to around 10km upstream of Schuylkill River, maximum storm surge is larger than the extreme water level except for some small patches around river boundaries. This indicates that the maximum storm surge coincided with the tide at the negative level over most part of the estuary, which have alleviated the effect of storm surge. However, further upstream to the head of the estuary at Trenton, the extreme water level is larger

than the maximum storm surge, owing to the increasing influence of the Delaware River on the water level.

[Insert Figure 8]

River discharge and local wind induced water level component

Figure 9a shows the spatial distribution of the simulated maximum of river discharge induced water level component. The influence of river discharge is mainly limited to the area upstream of Schuylkill River during Hurricane Isabel, with the maximum water level component of river larger than 0.2m. This area is also considered to be freshwater portion of the Delaware Estuary (Sharp, 1983; Sharp *et al.*, 1986). Downstream of this area to the mouth of the Delaware Estuary, the river induced water level maximum during Isabel is rather small (less than 0.1m). This implies that future forecast of extreme water level under similar condition may not need to consider river input's influence in lower part of the estuary.

The spatial distribution of local wind induced maximum water level is shown in Figure 9b. Compared to river discharge, local wind has a more pronounced effect on water level over the whole estuary. The wind induced water level component increases from less than 0.1m around the mouth to more than 0.3m upstream of Schuylkill River in the longitudinal direction. In addition, transverse variation of the wind induced water level can be observed downstream of Ship John Shoal, where the water level of New Jersey side is higher than that of the Delaware side. This is mainly associated with the dominating wind of Northerly to Northwesterly, which has caused the movement of the water out of the estuary to the Delaware side of the estuary. However, this lateral variation vanishes upstream with the narrowing of the channel.

[Insert Figure 9]

Model Uncertainty Analysis

In spite of the satisfactory results generated, there are several limitations with the model framework used in this study, which needs to be improved with further efforts.

First, the water level component induced by wave setup/set-down is missing. This component accounts for the positive/negative changes of water level induced by surface waves (Bowen *et al.*, 1968). According to Marsooli and Lin (2018), the maximum wave setup over

most regions of U.S. East coast during historical hurricanes from 1988 to 2015 is on the order of 0.1 m and can be larger than 0.25 m in shallow regions of Delaware Bay. However, due to the absence of a wave model in the model framework over Delaware Estuary, the influence of wave to water level cannot be resolved. Future efforts by coupling D-Flow FM with a wave model (e.g., Salehi, 2018), is expected to be conducted to improve model performance.

In addition, the nonlinear tidal-surge interaction is not separated from the storm surge induced water level. Non-linear interaction between tide and surge can significantly influence the timing and magnitude of storm surge (Rossiter, 1961). It has been observed that the tide-surge interaction induced maximum storm tide change (extreme water level change in this study) ranges from -15% to 16% at tidal gauges located along Northeastern U.S. coasts (Marsooli and Lin, 2018). In this case, a better understanding of the tide-surge interaction is of vital importance for a better forecast of total water level (Bernier and Thompson, 2007).

Besides, direct precipitation as well as grid spacing of model may also have some influence on the model results. A recent study conducted by Zhang *et al.*, (2020) over the Delaware Estuary during Hurricane Irene highlighted the noticeable impact (~25cm) of heavy precipitation (~10 inch/day) on the simulated water level in the upper estuary. Meanwhile they concluded that the influence of grid spacing on the simulation results is minimal (~0.2%). Further, future work by incorporating the ocean baroclinicity may further improve the simulation skills as demonstrated in Pringle *et al.*, (2019).

CONCLUSION

A model framework for extreme water level simulation in coastal areas during hurricane events is introduced in this study. The NWM serves as the hydrologic component to simulate rainfall-runoff process, providing river discharge information. D-Flow FM is responsible for simulating the hydrodynamic processes in the near-shore. ADCIRC is employed to provide ocean boundary conditions beyond the coastal transition zone. The model framework is tested on the Delaware Estuary during Hurricane Isabel (2003) to simulate the total and extreme water level and the relative contribution of different physical components.

Our results suggest that the model is able to reproduce the total water level and extreme water level with an average Willmott skill of 0.970 and 0.965, respectively. During Hurricane

Isabel, the maximum storm surge coincides with negative tide level over most of the Delaware Estuary, resulting extreme water level lower than the maximum storm surge. Component analysis reveals that storm surge dominates the extreme water level with an average contribution of 78.16%, followed by the astronomical tide (19.52%). The influence of the river discharge is mainly restricted to the upper part of the estuary upstream of the Schuylkill River, where river induced water level can be larger than 0.2 m. Downstream of that, the contribution of rivers is less than 0.1 m. Compared to riverine contribution, local wind induced water level is more pronounced over the whole estuary. It is 0.1m around Brandywine Shoal Light at the lower part of the estuary and quickly increases to be larger than 0.2m over most part of the Delaware Estuary.

In spite of the good performance, uncertainty exists in the model results as tide-surge interaction and wave setup/set-down is not considered in the current model. A better understanding of tide-surge interaction and the introduction of wave models into the current framework could further improve the model performance.

ACKNOWLEDGMENTS

This research was based on the work conducted during 2019 Consortium of Universities for the Advancement of Hydrologic Science Inc. (CUAHSI) National Water Center Innovators Program Summer Institute. Mr. Edward P. Clark, Director of the National Water Center & Deputy Director Office of Water Prediction and Dr. Trey Flowers, Director of the Analysis and Prediction Division at the National Water Center are thanked for their authorization of the use of the model framework presented in this study. This project was also partially funded by The Water Institute of the Gulf under project “Project Louisiana Rivers’ Sediment Flux to the Coastal Ocean using a Coupled Atmospheric-Hydrological Model” (award number RCEGR260003-01-00). This project was paid for (in part) with federal funding from the Department of the Treasury through the Louisiana Coastal Protection and Restoration Authority’s Center of Excellence Research Grants Program under the Resources and Ecosystems Sustainability, Tourist Opportunities, and Revived Economies of the Gulf Coast States Act of 2012 (RESTORE Act). The statements, findings, conclusions, and recommendations are those of the author(s) and do not necessarily reflect the views of the Department of the Treasury, CPRA or The Water Institute of the Gulf. This material is based upon work supported by the National Center for Atmospheric Research, which is a major facility sponsored by the National Science Foundation under Cooperative Agreement No. 1852977. Personal discussion with Yanda Ou and Daoyang Bao at Louisiana State University has improved the quality of the manuscript.

LITERATURE CITED

Arnold, J. G., Srinivasan, R., Muttiah, R. S., & Williams, J.R., 1998. Large Area Hydrologic Modeling and Assessment. Part I: Model Development. *Nutrition* 17:70.

- Bacopoulos, P., Y. Tang, D. Wang, and S.C. Hagen, 2017. Integrated Hydrologic-Hydrodynamic Modeling of Estuarine-Riverine Flooding: 2008 Tropical Storm Fay. *Journal of Hydrologic Engineering* 22:1–11.
- Bakhtyar, R., P. Velissariou, K. Maitaria, B. Trimble, T. Flowers, H. Mashriqui, S. Moghimi, A. Abdolali, A.J. Van der Westhuysen, and G.R. Aggett, 2019. Regional-Scale Hydrologic and Hydrodynamic Modeling of a Riverine-Estuarine System under Extreme Storms: Application to US East Coast. AGU Fall Meeting 2019.
- Bakhtyar, R., K. Maitaria, P. Velissariou, B. Trimble, H. Mashriqui, S. Moghimi, A. Abdolali, A.J. Van der Westhuysen, Z. Ma, E.P. Clark, and T. Flowers, 2020. A New 1D/2D Coupled Modeling Approach for a Riverine-Estuarine System Under Storm Events: Application to Delaware River Basin. *Journal of Geophysical Research: Oceans* 125. doi:10.1029/2019JC015822.
- Bernier, N.B. and K.R. Thompson, 2007. Tide-Surge Interaction off the East Coast of Canada and Northeastern United States. *Journal of Geophysical Research: Oceans* 112:1–12.
- Beven, J.L. and H. Cobb, 2003. Tropical Cyclone Report: Hurricane Isabel. Tropical Cyclone Report:30.
- Bilskie, M. V. and S.C. Hagen, 2018. Defining Flood Zone Transitions in Low-Gradient Coastal Regions. *Geophysical Research Letters* 45:2761–2770.
- Bowen, A.J., D.L. Inman, and V.P. Simmons, 1968. Wave ‘Set-down’ and Set-Up. *Journal of Geophysical Research* 73:2569–2577.
- Deltares, 2019a. Delft3D Flexible Mesh Suite.
- Deltares, 2019b. 3D/2D Modelling Suite for Integral Water Solutions: Hydro-Morphodynamics. :710.
- Disasters, Centre for Research on the Epidemiology of Reduction, U.N.O. for D.R., 2015. The Human Cost of Weather-Related Disasters 1995-2015. :2–4.
- Dresback, K.M., J.G. Fleming, B.O. Blanton, C. Kaiser, J.J. Gourley, E.M. Tromble, R.A. Luettich, R.L. Kolar, Y. Hong, S. Van Cooten, H.J. Vergara, Z.L. Flamig, H.M. Lander, K.E. Kelleher, and K.L. Nemunaitis-Monroe, 2013. Skill Assessment of a Real-Time Forecast System Utilizing a Coupled Hydrologic and Coastal Hydrodynamic Model during Hurricane Irene (2011). *Continental Shelf Research* 71:78–94.
- Gochis, D.J., M. Barlage, A. Dugger, K. Fitzgerald, L. Karsten, M. Mcallister, J. McCreight, J. Mills, A. Rafiecinasab, L. Read, K. Sampson, D. Yates, and W. Yu, 2018. WRF-Hydro V5 Technical Description Originally Created : Updated : WRF-Hydro V5 Technical Description. NCAR Technical Note.
- Koren, V., S. Reed, M. Smith, Z. Zhang, and D.J. Seo, 2004. Hydrology Laboratory Research Modeling System (HL-RMS) of the US National Weather Service. *Journal of Hydrology* 291:297–318.
- Lin, N., J.A. Smith, G. Villarini, T.P. Marchok, and M.L. Baeck, 2010. Modeling Extreme Rainfall, Winds, and Surge from Hurricane Isabel (2003). *Weather and Forecasting* 25:1342–1361.
- Luettich, R.A., J.J. Westerink, and N.W. Scheffner, 1993. ADCIRC: An Advanced Three-Dimensional Circulation Model for Shelves Coasts and Estuaries, Report 1: Theory and Methodology of ADCIRC-2DDI and ADCIRC-3DL, Dredging Research Program Technical Report DRP-92-6.
- Marsooli, R. and N. Lin, 2018. Numerical Modeling of Historical Storm Tides and Waves and Their Interactions along the U.S. East and Gulf Coasts. *Journal of Geophysical Research: Oceans* 123:3844–3874.
- McKay, L., T. Bondelid, T. Dewald, J. Johnston, R. Moore, and A. Rea, 2019. NHDPlus Version 2: User Guide

(Data Model Version 2.1). :182.

- Merz, B., J. Hall, M. Disse, and A. Schumann, 2010. Fluvial Flood Risk Management in a Changing World. *Natural Hazards and Earth System Science* 10:509–527.
- Moftakhari, H.R., A. AghaKouchak, B.F. Sanders, D.L. Feldman, W. Sweet, R.A. Matthew, and A. Luke, 2015. Increased Nuisance Flooding along the Coasts of the United States Due to Sea Level Rise: Past and Future. *Geophysical Research Letters* 42:9846–9852.
- Moftakhari, H.R., G. Salvadori, A. AghaKouchak, B.F. Sanders, and R.A. Matthew, 2017. Compounding Effects of Sea Level Rise and Fluvial Flooding. *Proceedings of the National Academy of Sciences of the United States of America* 114:9785–9790.
- Moftakhari, H., J.E. Schubert, A. AghaKouchak, R.A. Matthew, and B.F. Sanders, 2019. Linking Statistical and Hydrodynamic Modeling for Compound Flood Hazard Assessment in Tidal Channels and Estuaries. *Advances in Water Resources* 128:28–38.
- Muñoz, D.F., D.X. Yin, R. Bakhtyar, H. Moftakhari, Z. Xue, K. Mandli, and C. Ferreira, 2020. Inter-model comparison of Delft3D-FM and 2D HEC-RAS for Total Water Level Prediction in Coastal to Inland Transition Zones. *JAWRA Journal of the American Water Resources Association*. Under review.
- National Data Buoy Center, . <https://www.ndbc.noaa.gov/>. Accessed 14 Feb 2020.
- Niu, G.Y., Z.L. Yang, K.E. Mitchell, F. Chen, M.B. Ek, M. Barlage, A. Kumar, K. Manning, D. Niyogi, E. Rosero, M. Tewari, and Y. Xia, 2011. The Community Noah Land Surface Model with Multiparameterization Options (Noah-MP): 1. Model Description and Evaluation with Local-Scale Measurements. *Journal of Geophysical Research Atmospheres* 116:1–19.
- NOAA/NOS's VDatum 4.0.1: Vertical Datums Transformation, . <https://vdatum.noaa.gov/>. Accessed 14 Feb 2020.
- NOAA Tides and Currents, . <https://www.tidesandcurrents.noaa.gov/>. Accessed 14 Feb 2020.
- Pringle, W.J., J. Gonzalez-Lopez, B.R. Joyce, J.J. Westerink, and A.J. van der Westhuysen, 2019. Baroclinic Coupling Improves Depth-Integrated Modeling of Coastal Sea Level Variations Around Puerto Rico and the U.S. Virgin Islands. *Journal of Geophysical Research: Oceans* 124:2196–2217.
- Rafieeinasab, A., L. Karsten, A. Dugger, K. Fitzgerald, R. Cabell, D. Gochis, D. Yates, K. Sampson, J. McCreight, L. Read, Y. Zhang, and M. McCallister, 2020. Overview of National Water Model Calibration General Strategy & Optimization.
- Rossiter, J.R., 1961. Interaction Between Tide and Surge in the Thames. *Geophysical Journal of the Royal Astronomical Society* 6:29–53.
- Saharia, M., P.-E. Kirstetter, H. Vergara, J.J. Gourley, Y. Hong, and M. Giroud, 2017. Mapping Flash Flood Severity in the United States. *Journal of Hydrometeorology* 18:397–411.
- Salehi, M., 2018. Storm Surge and Wave Impact of Low-Probability Hurricanes on the Lower Delaware Bay-Calibration and Application. *Journal of Marine Science and Engineering* 6. doi:10.3390/jmse6020054.
- Sharp, J.H., 1983. The Delaware Estuary: Research as Background for Estuarine Management and Development. Delaware River and Bay Authority Report:326 pp.
- Sharp, J.H., L.A. Cifuentes, R.B. Coffin, J.R. Pennock, and K.C. Wong, 1986. The Influence of River Variability on

- the Circulation, Chemistry, and Microbiology of the Delaware Estuary. *Estuaries* 9:261–269.
- Sheng, Y.P., V. Alymov, and V.A. Paramygin, 2010. Simulation of Storm Surge, Wave, Currents, and Inundation in the Outer Banks and Chesapeake Bay during Hurricane Isabel in 2003: The Importance of Waves. *Journal of Geophysical Research: Oceans* 115. doi:10.1029/2009JC005402.
- Ters, L.E.T., 2016. Compound Hazards Yield Louisiana Flood Addressing Obesity in Homeless Children Zika Vaccine : Clinical Trial and Error ?
- The Climate Data Guide: Climate Forecast System Reanalysis (CFSR) National Center for Atmospheric Research Staff (Eds), .
- USGS Water Data for the Nation, . <https://waterdata.usgs.gov/nwis>. Accessed 14 Feb 2020.
- Walters, R.A., 1997. A Model Study of Tidal and Residual Flow in Delaware Bay and River. *Journal of Geophysical Research: Oceans* 102:12689–12704.
- Wdowinski, S., R. Bray, B.P. Kirtman, and Z. Wu, 2016. Increasing Flooding Hazard in Coastal Communities Due to Rising Sea Level: Case Study of Miami Beach, Florida. *Ocean and Coastal Management* 126:1–8.
- Webster, P.J., G.J. Holland, J.A. Curry, and H.R. Chang, 2005. Atmospheric Science: Changes in Tropical Cyclone Number, Duration, and Intensity in a Warming Environment. *Science* 309:1844–1846.
- Willmott, C.J., 1981. On the Validation of Models. *Physical Geography* 2:184–194.
- Wing, O.E.J., P.D. Bates, A.M. Smith, C.C. Sampson, K.A. Johnson, J. Fargione, and P. Morefield, 2018. Estimates of Present and Future Flood Risk in the Conterminous United States. *Environmental Research Letters* 13. doi:10.1088/1748-9326/aaac65.
- Winsemius, H.C., J.C.J.H. Aerts, L.P.H. Van Beek, M.F.P. Bierkens, A. Bouwman, B. Jongman, J.C.J. Kwadijk, W. Ligtvoet, P.L. Lucas, D.P. Van Vuuren, and P.J. Ward, 2016. Global Drivers of Future River Flood Risk. *Nature Climate Change* 6:381–385.
- Woodruff, J.D., J.L. Irish, and S.J. Camargo, 2013. Coastal Flooding by Tropical Cyclones and Sea-Level Rise. *Nature* 504:44–52.
- Zhang, Y.J., F. Ye, H. Yu, W. Sun, S. Moghimi, E. Myers, K. Nunez, R. Zhang, H. Wang, A. Roland, J. Du, and Z. Liu, 2020. Simulating Compound Flooding Events in a Hurricane. *Ocean Dynamics* 70:621–640.

TABLE 1. Setup of the experiments with different scenarios

Exp.	River	Astronomical tide	Storm Surge	Local Wind and Atmospheric Pressure	Water level components	Model Component Used
E1	N/A	Y	N/A	N/A	Astronomical Tide	D-Flow FM + ADCIRC
E2	Y	Y	N/A	N/A	Astronomical Tide +	D-Flow FM +

					River discharge induced water level	NWM
E3	N/A	Y	N/A	Y	Astronomical Tide + Local wind forcing induced water level	D-Flow FM + CFSR
E4	Y	Y	Y	Y	Total water level	D-Flow FM + NWM + CFSR + ADCIRC

TABLE 2. Transformation relationship between NAVD88 and MSL

CO-OPS Gauge	NAVD88-MSL(m)
Brandywine Shoal Light	0.091
Ship John Shoal	0.039
Marcus Hook	-0.049
Burlington	-0.180
Newbold	-0.161

Figure 1. (a) Schematic structure of the numerical framework. (b) NOAA best track for Hurricane Isabel with 6 hours interval, study area is outlined with the red box. (c) Study area and

computational domain of the model framework. Overview map at the top right corner indicates the location of the study area. D-Flow FM domain is in yellow, beyond it at the ocean side oceanic processes are calculated by ADCIRC while hydrological processes are simulated by NWM at land side. Observation stations used in this study are also shown.

Figure 2. Time series of simulated (red lines) astronomical tides and NOAA prediction (black lines) at (a) Cape May, (b) Lewes, (c) Brandywine Shoal Light, (d) Ship John Shoal, (e) Marcus Hook, (f) Burlington and (g) Newbold.

Figure 3. Comparisons between CFSR (red) and observed (black) (a) wind speed, (b) wind direction, and (c) atmospheric pressure. The arrow of the wind direction points to the direction where wind blows to. The blue dash line indicates the landfall time of Hurricane Isabel (2003).

Figure 4. Simulated (red) and observed (black) discharge at (a) Delaware River and (b) Schuylkill River. The blue dash line indicates the landfall time of Hurricane Isabel (2003). Note that observation data for river discharge of Delaware River is not available during September 10 to September 15, 2003.

Figure 5. Time series of simulated (red lines) total water level and observation (black lines) at (a) Cape May, (b) Lewes, (c) Brandywine Shoal Light, (d) Ship John Shoal, (e) Marcus Hook, (f) Burlington and (g) Newbold. The blue dash line indicates the landfall time of Hurricane Isabel.

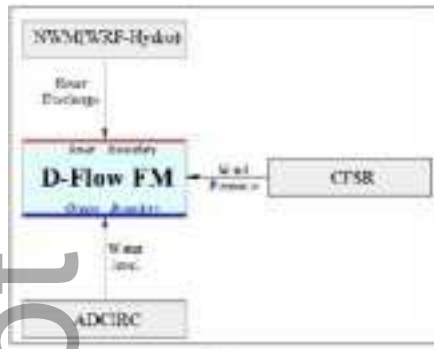
Figure 6. Simulated and observed extreme water level at selected CO-OPS gauges.

Figure 7. The water level components of extreme water level induced by Astronomical Tide (AT), River Discharge (River), Storm Surge(SS) at selected NOAA tide gauge stations: Cape May(1), Lewes(2), Brandywine Shoal Light (3), Ship John Shoal(4), Marcus Hook (5), Burlington(6) and Newbold(7). The value of each component and total water level (TWL) is also attached. The unit is meter. The locations of the tide gauge stations are shown in Figure 1c.

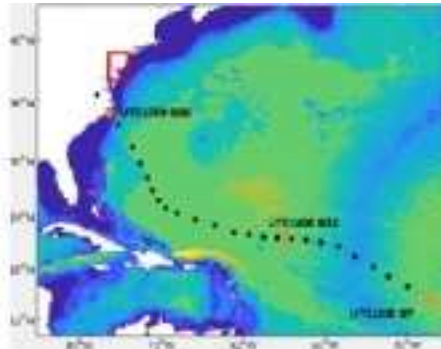
Figure 8. Spatial distribution of extreme water level (a), maximum storm surge induced water level (b), and the difference map (c)=(a)-(b), over Delaware Estuary. Black dots represent the locations of river boundaries in the model framework.

Figure 9. Spatial distribution of simulated maximum water level induced by (a) river discharge and (b) local wind over study area. Pink dots represent the location of river boundaries and red triangles indicate the selected CO-OPS gauges in the model framework.

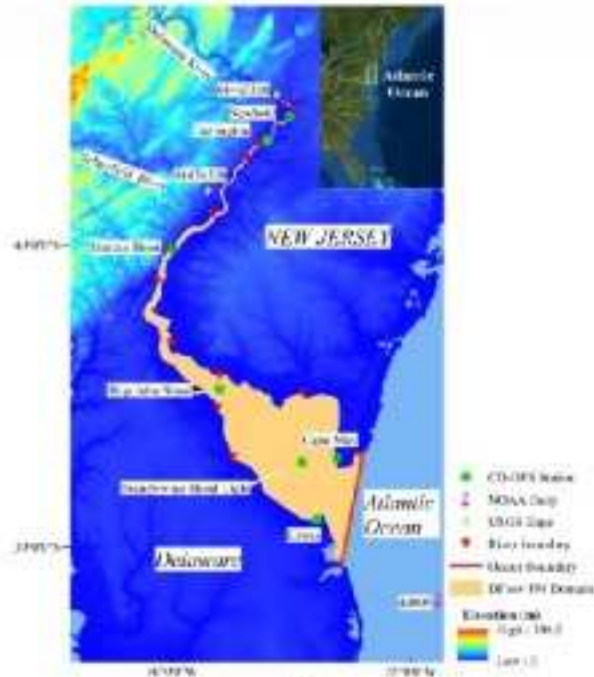
Author Manuscript



(a)

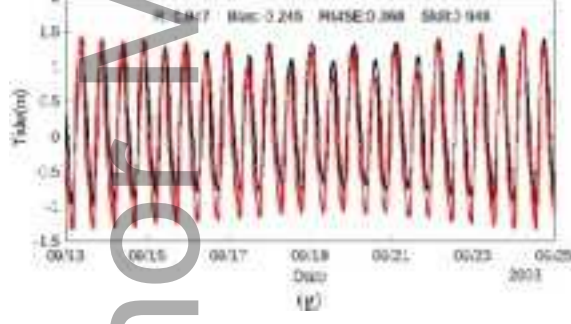
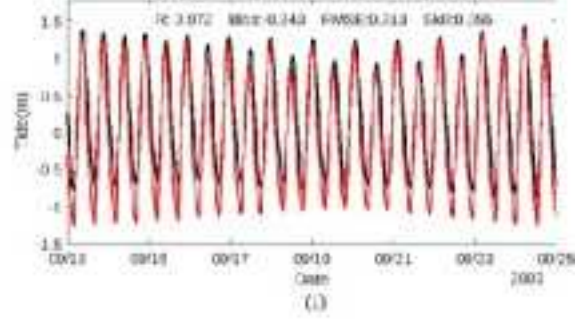
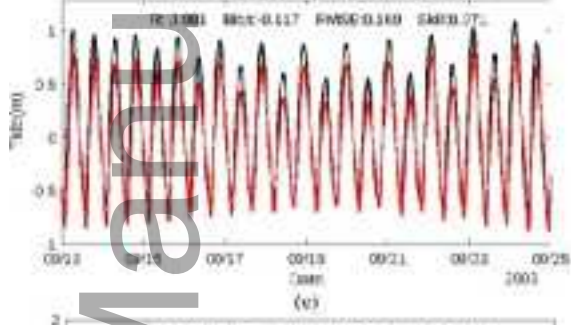
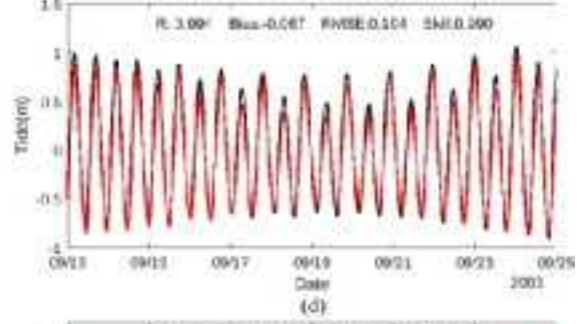
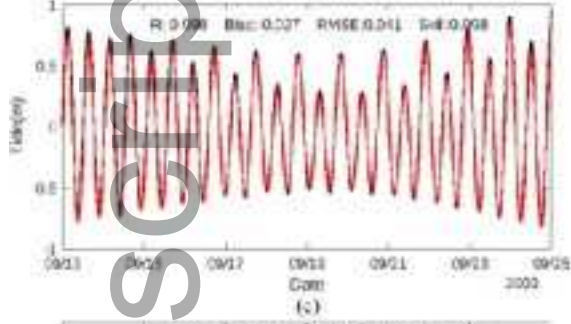
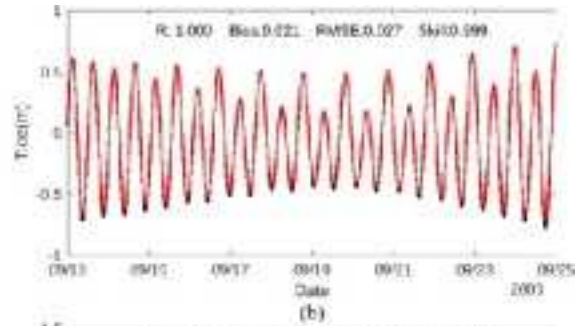
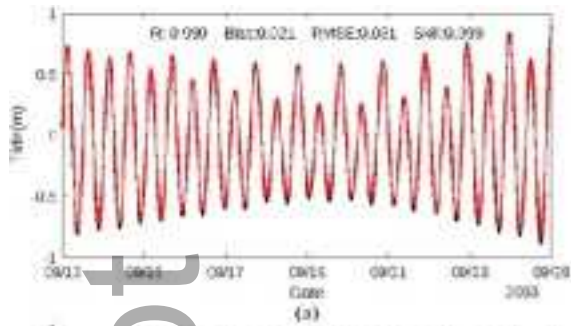


(b)

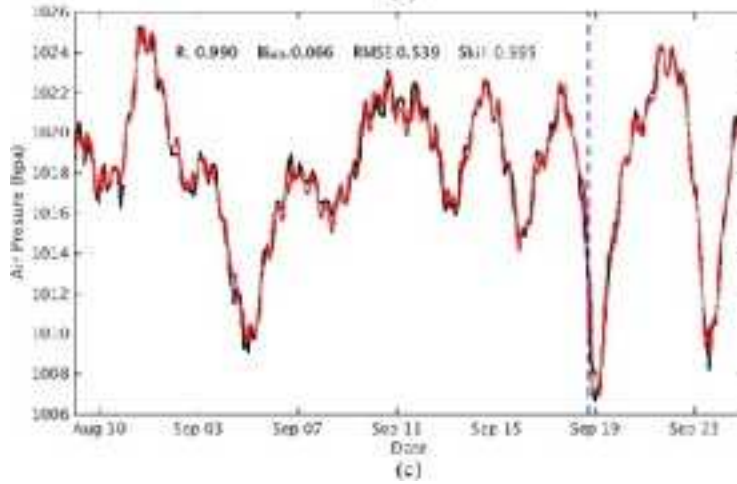
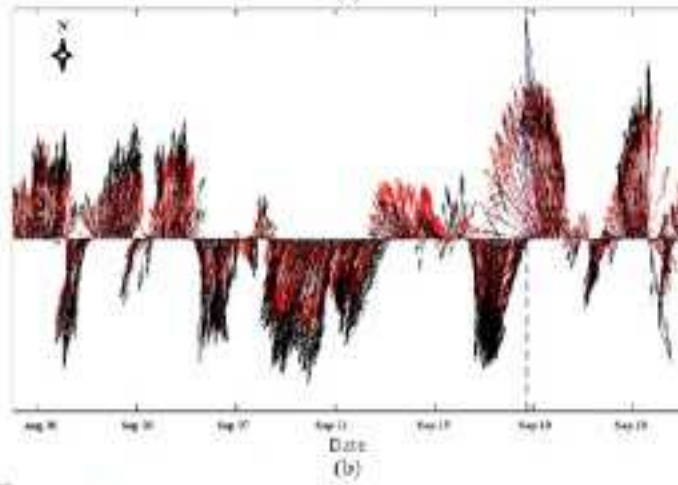
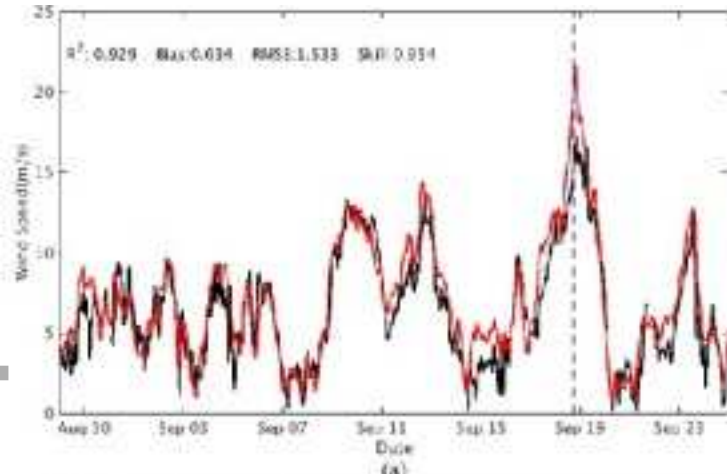


(c)

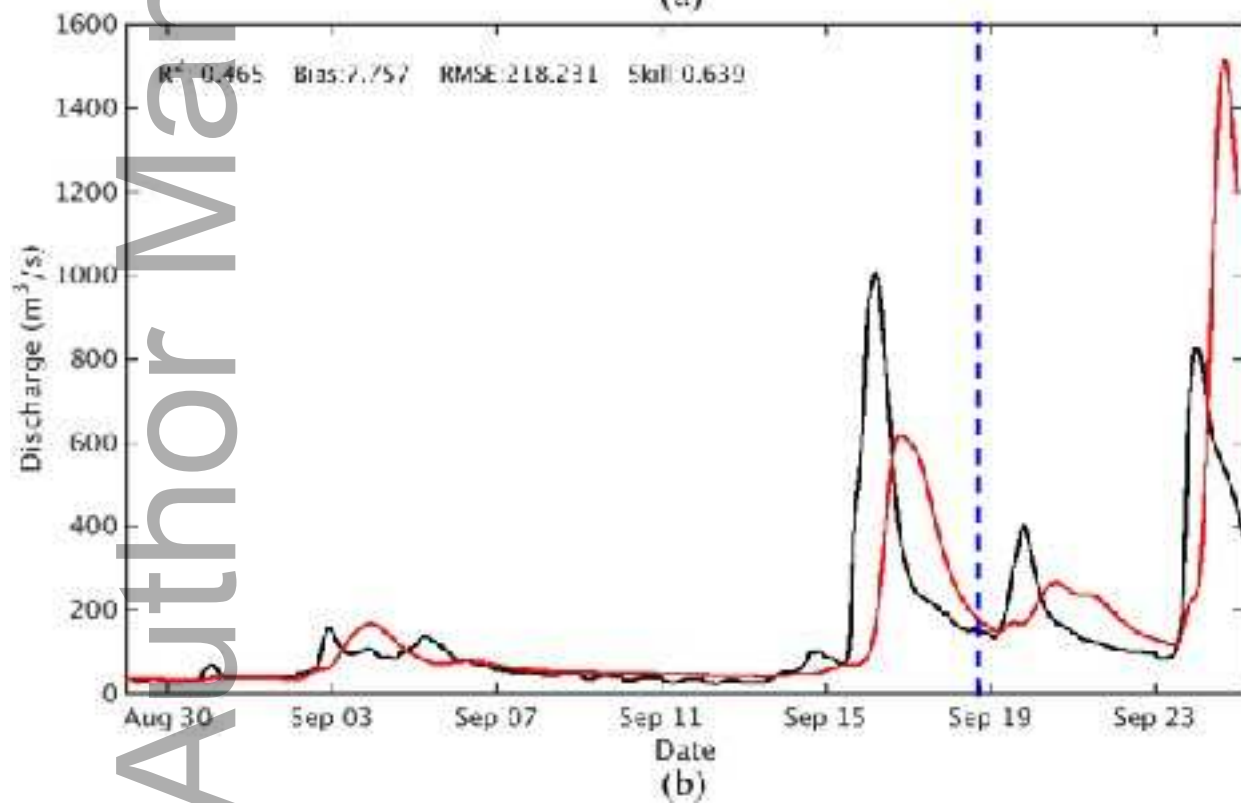
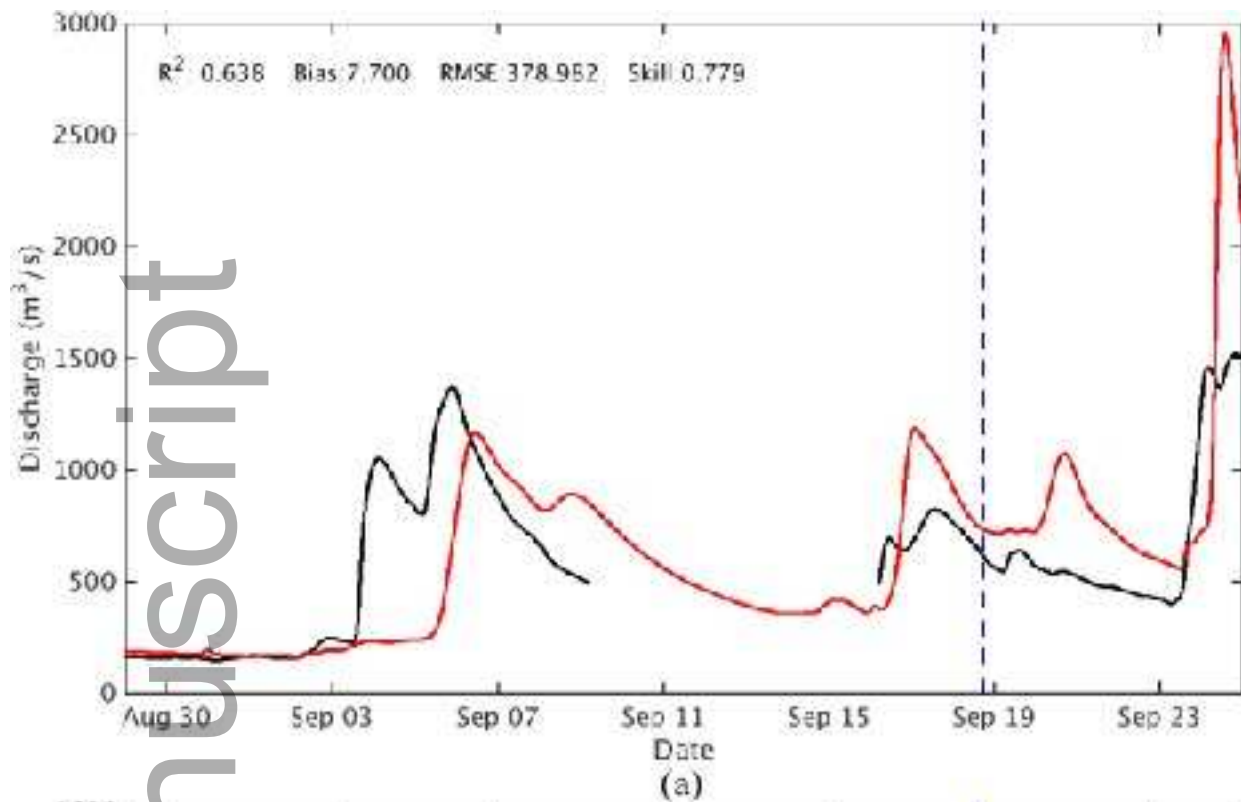
jawr_12947_f1.tiff



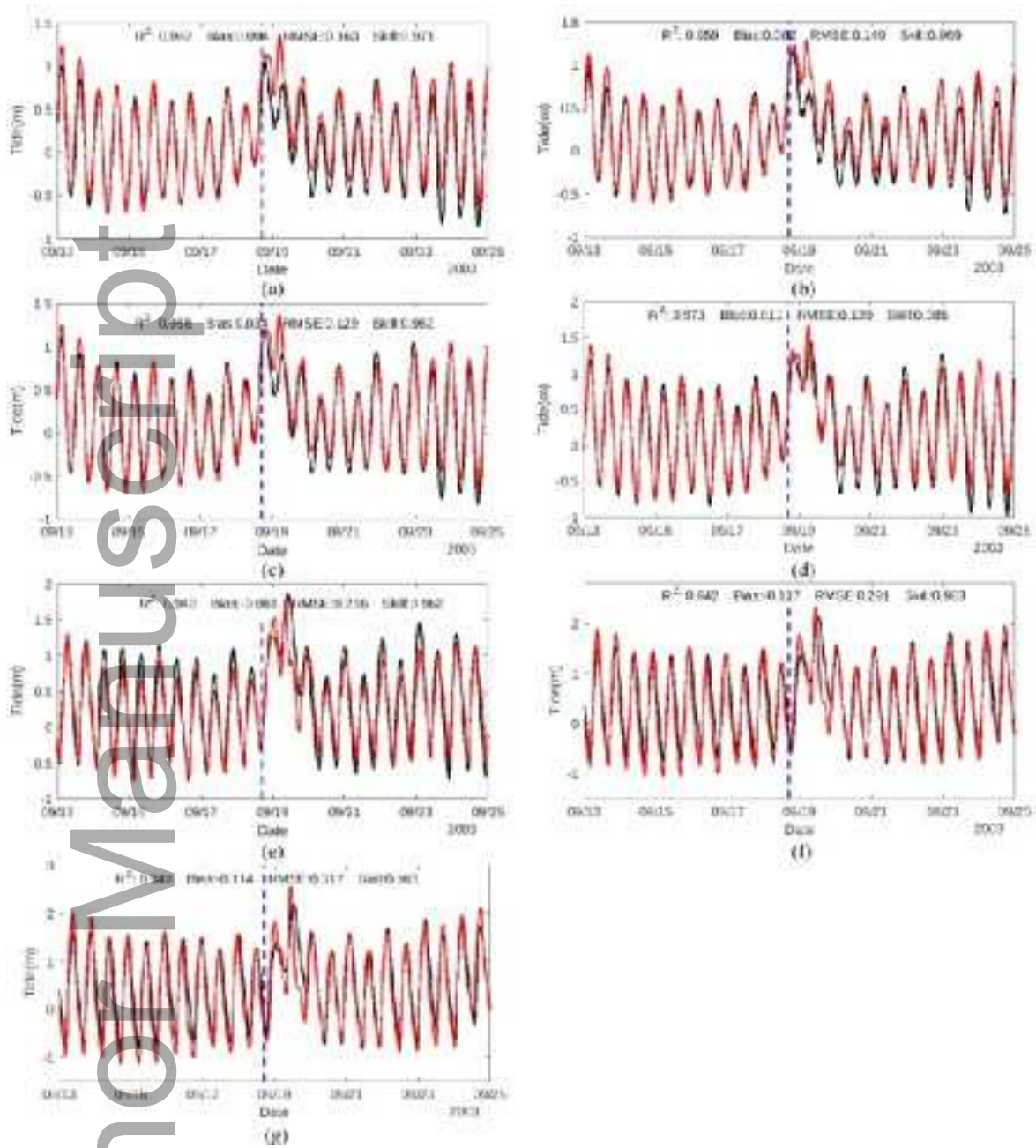
jawr_12947_f2.tiff



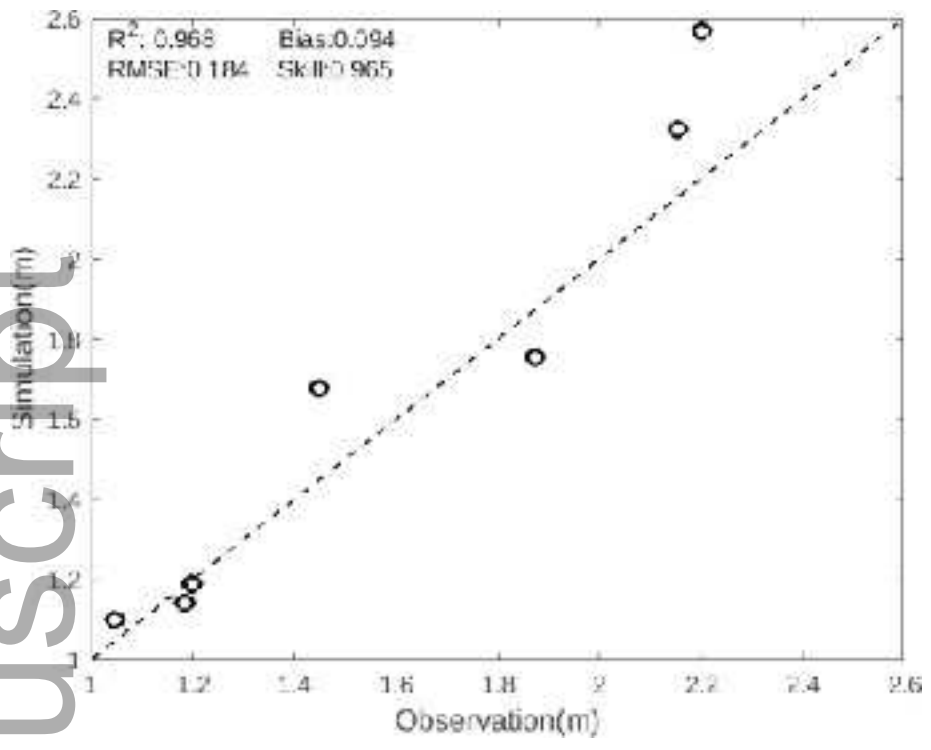
jawr_12947_f3.tiff



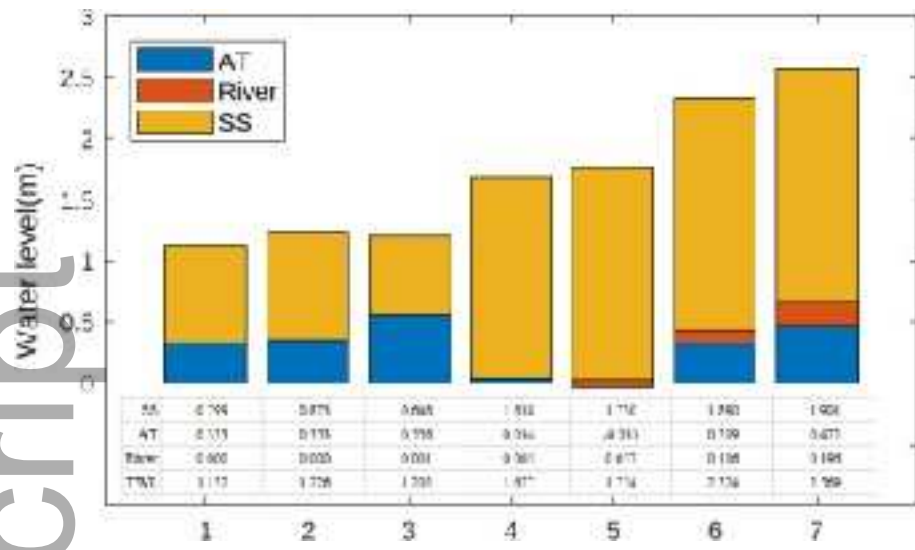
jawr_12947_f4.tiff



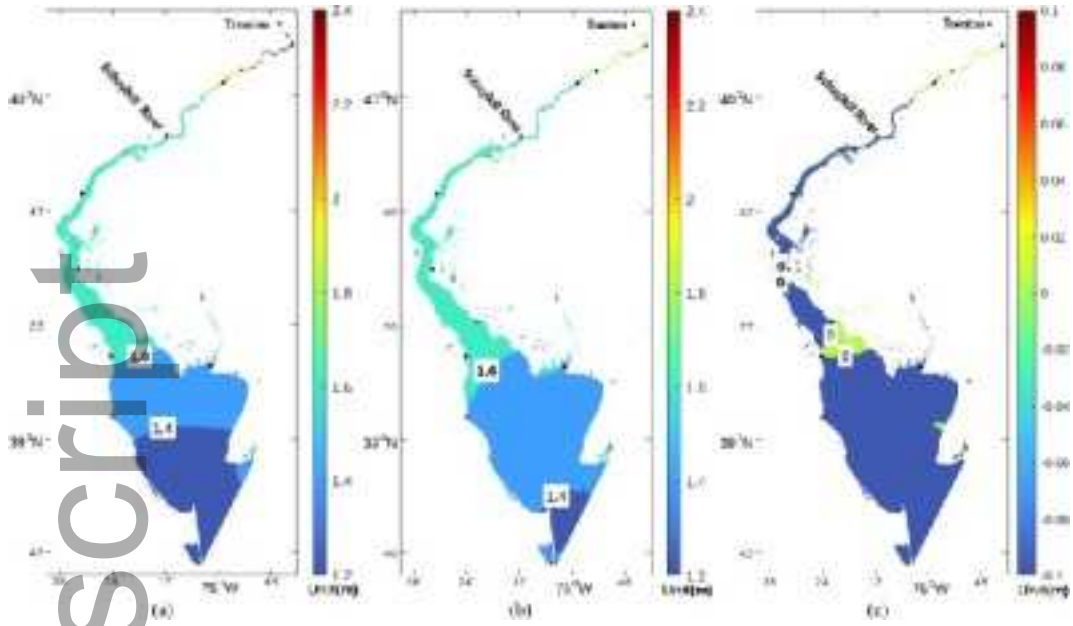
jawr_12947_f5.tiff



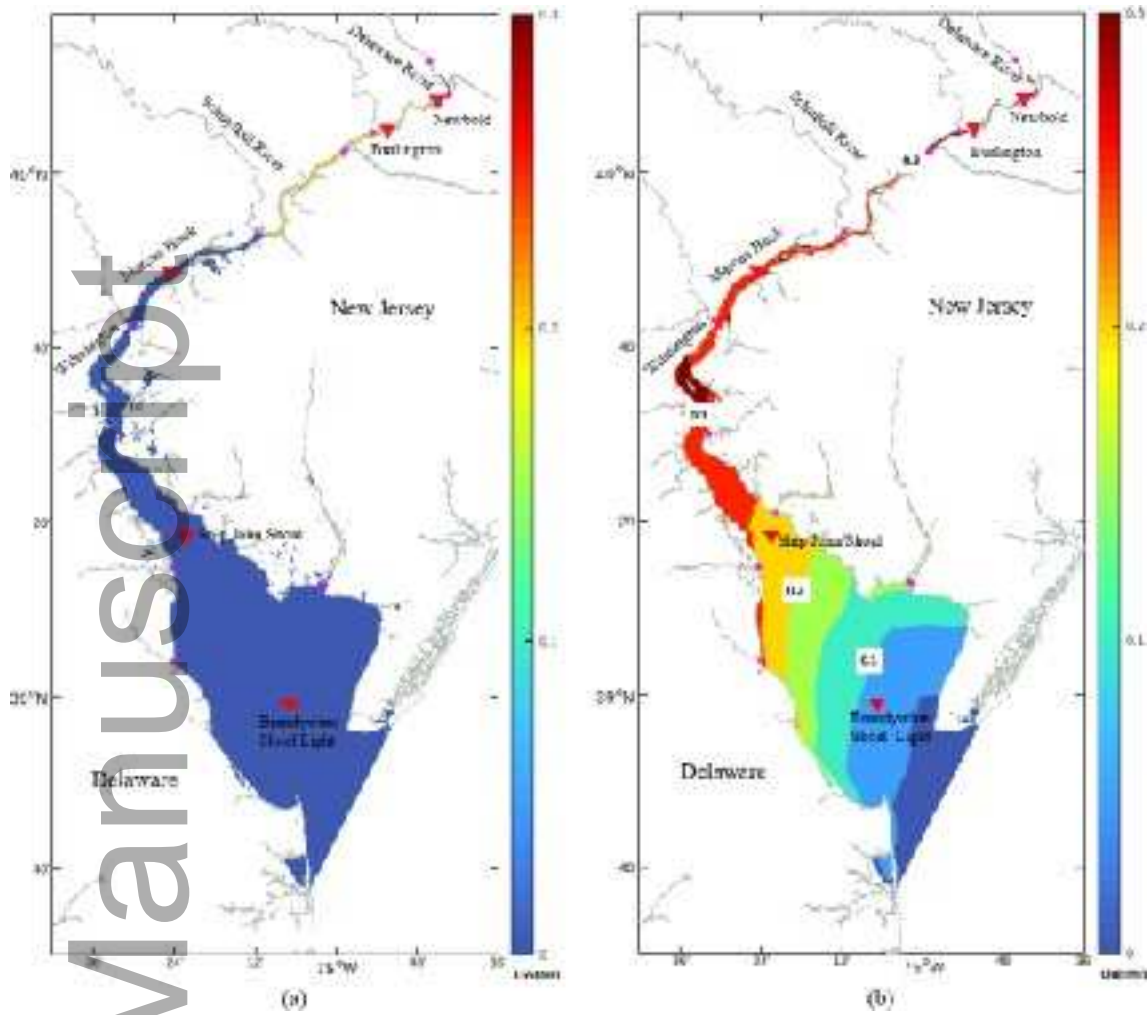
jawr_12947_f6.tiff



jawr_12947_f7.tiff



jawr_12947_f8.tiff



jawr_12947_f9.tiff